Supporting Information

Axial Ligand Effects on the Geometric and Electronic Structures of Nonheme Oxoiron(IV) Complexes

Timothy A. Jackson[†,‡], Jan-Uwe Rohde[†,#] , Mi Sook Seo[§], Chivukula V. Sastri[§], Raymond DeHont[□], Takehiro Ohta[⊥], Teizo Kitagawa[⊥], Eckard Münck[□,*], Wonwoo Nam[§,*], and Lawrence Que Jr.[†,*]

[†] University of Minnesota.

[‡] Current address: Department of Chemistry, University of Kansas, Lawrence, KS 66045.

[#] Current address: Department of Chemistry, The University of Iowa, Iowa City, IA 52242.

[§]Ewha Womans University.

[□]Carnegie Mellon University.

[⊥]National Institutes of Natural Sciences.

Experimental Details. A) EXAFS Fitting Details for 1-OH and 1-NCS; B) Badger's Rule Analysis of Fe=O Vibrations; and C) Evaluation of Functionals for TD-DFT Computations.

Experimental Details.

A. EXAFS Fitting Details for 1-OH and 1-NCS. For the $[Fe^{IV}(O)(TMC)(OH)]^+$ sample, the inclusion of a third inner shell at 1.94 Å appreciably decreased the *F* value from 1.04 to 0.79 but caused an increase in the σ^2 value of the innermost O shell (termed σ^2(Fe–O)) from 0.0013 to 0.0033 Å^2 and a decrease in the σ^2 value of the N shell (termed σ^2(Fe–N)) from 0.0045 to 0.0017 Å^2 (Table S2). Additionally, the shell at 1.94 Å exhibited a σ^2 value of -0.0013, which is unusually small for a shell at this distance. Together, these observations might initially suggest that the shell at 1.94 Å be eliminated from our fitting analysis. However, inspection of the correlation matrices for these fits revealed large correlations for the σ^2 values of the inner shells (0.86 – 0.88). To evaluate the consequence of these correlations on the EXAFS fitting, the σ^2 value of the shell at 1.94 Å (termed σ^2(Fe–OH)) was systematically varied from 0.003 to -0.003 Å^2 in 0.0005 Å^2 increments. As shown in Table S3 and Figure S3, when σ^2(Fe–OH) is varied from -0.0005 to 0.003 Å^2, the *F* value only increases by 13 (~6%), and the iron–scatterer distances remain essentially constant, whereas σ^2(Fe–O) and σ^2(Fe–N) decrease and increase appreciably. Consequently, if σ^2(Fe–OH) is fixed at a reasonable value of 0.002 Å^2, then σ^2(Fe–O) and σ^2(Fe–N) are 0.0012 and 0.0026 Å^2, respectively, values similar to those observed in the absence of the Fe–OH shell (Table S2). On the basis of these observations, the inclusion of this shell thus appears warranted.

In fact, assuming an Fe–N distance of 2.0 Å for the NCS^- ligand, an Fe···S distance of ~4.8 Å is predicted. While the inclusion of a S scatterer at ~5 Å reduced the GOF value by ~28% (Table S2), this shell has a very small, negative Debeye-Waller factor of -0.0011 Å^2, which suggests an unrealistically high degree of order. Accordingly, we re-fit these data using multiple-scattering paths obtained from the program *FEFF* and a model of the **1**-NCS complex derived from density functional theory (DFT) energy minimization (*vide infra*). The *FEFF* analysis predicted four prominent multiple-scattering paths associated with the linear Fe–NCS unit. Inclusion of these paths led to more reasonable fits (Table 3).

B. Badger's Rule Analysis of Fe=O Vibrations. The $^{16}O/^{18}O$ isotopic shifts of ν_{FeO} for 1-NCMe and all members of the 1-X series are close to the calculated value for an Fe–O diatomic oscillator (-33 cm^{-1}), implying nearly pure Fe–O vibrations. Accordingly, the ν_{FeO} energy should be indicative of the Fe–O bond length. The two may in fact be correlated via Badger's rule, which relates these observables through the relatively simple equation $r_e = C_{ij} / \nu_e^{2/3} + d_{ij}$, where r_e and ν_e are the equilibrium Fe–O distance and stretching frequency, respectively, and C_{ij} and d_{ij} are empirical constants typically determined by fitting r_e and ν_e values for a series of complexes.[1] Green has demonstrated the applicability of Badger's rule for a relatively large number of oxoiron species and determined C_{ij} and d_{ij} values of 55.702 and 1.003, respectively.[1] Using those values for **1**-NCMe (ν_{FeO} = 839 cm^{-1}), an Fe–O distance of 1.629 Å is predicted, which underestimates the crystallographically determined distance (1.646 Å) by only 0.017 Å. By applying the Badger's rule correlation to the ν_{FeO} energies for **1**-O_2CCF_3 and **1**-N_3, which are the extremes of the TMC **1**-X series, respective bond lengths of 1.622 and 1.642 Å are predicted. The key parameter of comparison is the difference in predicted bond lengths, as this demonstrates that the shift of 40 cm^{-1} in Fe–O stretching frequency between **1**-O_2CCF_3 and **1**-N_3 may only correspond to a change in Fe–O bond length of 0.02 Å.

C. Evaluation of Functionals for TD-DFT Computations. We used the pure BP86 functional and the hybrid B3LYP and PBE0 functionals to determine which method most closely reproduces the experimental transition energies reported by Decker *et al*.[2] Computations performed with each of the three functionals predict a low-energy band (band *i*, see Figures 9 and S6) of moderate intensity that corresponds to the prominent NIR band of **1**-NCMe that appears in the experimental spectrum at 824 nm (Figure 2). Experimentally, this NIR band contains contributions from three distinct Fe^{IV} d → d transitions, of which the $d_{xz/yz} \rightarrow d_{x^2-y^2}$ transitions carry the most absorption intensity.[2] The $d_{xy} \rightarrow d_{x^2-y^2}$ and $d_{xy} \rightarrow d_{xz/yz}$ transitions contribute to the lower-energy shoulder of the absorption band at 824 nm, as they were observed at 960 and 940 nm (10 400 and 10 600 cm^{-1}), respectively.[2,3] For all three functionals, the low energy band computed by the TD-DFT method is due to the $d_{xz/yz} \rightarrow d_{x^2-y^2}$

transitions (Tables 6 and S13), (Note that Because the 1-NCMe complex does not have strict C_{4v} symmetry, the Fe^{IV} d_{xz} and d_{yz} MOs are nondegenerate. However, for most **1**-X complexes, these orbitals have very similar energies and thus will be referred to together unless otherwise noted.) in good agreement with the experimental data. In addition, computations performed using the hybrid functionals properly reproduce the experimental ordering of these three low-energy LF transitions (Table S13). Notably, the BP86 functional does not, as it predicts the $d_{xy} \rightarrow d_{xz/yz}$ transition to be at lower energy than the $d_{xy} \rightarrow d_{x^2-y^2}$ transition, in contrast to the experimental observations.[2,3] Thus, we will focus our discussion on the hybrid functionals, particularly the PBE0 functional, as it does a slightly better job of reproducing the proper absorption intensity over the B3LYP functional (Figure S7).

References

1. Green, M. T. Application of Badger's Rule to Heme and Non-Heme Iron-Oxygen Bonds: An Examination of Ferry Protonation States *J. Am. Chem. Soc.* **2006**, *128*, 1902-1906.
2. Decker, A.; Rohde, J.-U.; Que, L. J.; Solomon, E. I. Spectroscopic and Quantum Chemical Characterization of the Electronic Structure and Bonding in a Non-Heme Fe^{IV}=O Complex *J. Am. Chem. Soc.* **2004**, *126*, 5378-5379.
3. Decker, A.; Clay, M. D.; Solomon, E. I. Spectroscopy and electronic structures of mono- and binuclear high-valent non-heme iron-oxo systems *J. Inorg. Biochem.* **2006**, *100*, 697-706.

Table S1. EXAFS Fitting Results for $[Fe^{IV}(O)(TMC)(NCMe)]^{2+}$ (**1**-NCMe).[a]

		Fe–O			Fe–N			Fe···C			Fe···X			
complex	fit	*n*	*r*(Å)	σ^2	*n*	*r*(Å)	σ^2	*n*	*r*(Å)	σ^2	*n*	*r*(Å)	σ^2	*F*
1-NCMe[b]	1				6	2.07	6.8							1.31
	2	1	1.64	3.8	5	2.08	5.8							0.68
	3	**1**	**1.64**	**3.8**	**5**	**2.09**	**5.8**	**4**	**2.97**	**6.6**				**0.22**
	4	1	1.64	3.8	5	2.08	5.8	6	2.97	9.3				0.18
	6	*1*	*1.64*	*3.8*	*5*	*2.08*	*5.7*	*4*	*2.97*	*6.5*				*0.20*[c]
1-NCMe[d]					6	2.10	7.5							1.33
					5	2.10	5.9							1.24
		1	1.64	4.0	5	2.09	5.9							0.96
		1	1.64	3.8	5	2.09	5.9	4	2.97	1.7				0.76
		1	**1.64**	**3.8**	**5**	**2.09**	**5.9**	**6**	**2.97**	**4.5**				**0.84**

[a]Fourier-transform range is 2 – 15 $Å^{-1}$ (resolution 0.12 Å). σ^2 is in units of 10^3 $Å^2$. [b]EXAFS data fit using the program EXAFSPAK in conjunction with FEFF 6 and the back-transformation range 0.9 – 3.4 Å. [c]Fits to unfiltered data corresponding to best fits to filtered data. [d]EXAFS data fit using the program SSEXAFS and the back-transformation range 0.7 – 3.2 Å.

Table S2. EXAFS Fitting Results for $[Fe^{IV}(O)(TMC)(X)]^+$ (**1**-X), where X = $F_3CCO_2^-$, NCO^-, NCS^-, N_3^-, CN^-, OH^-.[a]

		Fe–O			Fe–N			Fe···C			Fe···X			
complex	fit	*n*	*r*(Å)	σ^2	*n*	*r*(Å)	σ^2	*n*	*r*(Å)	σ^2	*n*	*r*(Å)	σ^2	*F*[c]
1-O_2CCF_3[b]	1				5	2.09	3.4							1.37
	2	1	1.64	1.8	5	2.08	3.4							0.92
	3	**1**	**1.64**	**1.7**	**5**	**2.08**	**3.3**	**4**	**2.95**	**5.0**				**0.76**
	4	*1*	*1.64*	*2.0*	*5*	*2.08*	*3.5*	*4*	*2.95*	*5.4*				*0.79*[c]
1-NCO[d]	1				6	2.02	7.5							1.39
	2	1	1.65	1.8	5	2.07	7.2							0.49
	3	1	1.65	1.8	5	2.07	7.1	4	2.93	6.5				0.16
	4	**1**	**1.65**	**1.8**	**5**	**2.07**	**7.1**	**5**	**2.94**	**8.1**				**0.15**
	5	1	1.65	1.8	5	2.07	7.1	6	2.94	9.7				0.16
	6	*1*	*1.67*	*1.7*	*5*	*2.07*	*7.1*	*5*	*2.94*	*8.1*				*0.13*[c]
1-NCS[d]	1				6	2.03	5.0							1.79
	2	1	1.65	2.6	5	2.07	4.3							0.88
	3	1	1.65	2.7	5	2.07	4.3	4	2.95	4.3				0.63
	4	1	1.65	2.6	5	2.07	4.3	6	2.95	6.9				0.68
	5	1	1.65	2.6	5	2.07	4.3	4	2.95	4.3	1	4.61	-1.1	0.44
	6	**1**	**1.65**	**2.6**	**5**	**2.07**	**4.3**	**4**	**2.95**	**4.2**	**4**[e]	**4.78**	**5.4**	**0.45**
	7	*1*	*1.65*	*2.6*	*5*	*2.07*	*4.3*	*4*	*2.95*	*4.2*	*4*[e]	*4.78*	*5.4*	*0.21*[c]
1-N_3[d]	1				6	2.14	9.3							2.73
	2	1	1.66	2.1	5	2.08	6.5							0.64
	3	1	1.66	2.1	5	2.08	6.4	4	2.99	9.2				0.36
	4	**1**	**1.66**	**2.1**	**5**	**2.08**	**6.4**	**6**	**2.99**	**11.7**				**0.33**
	6	*1*	*1.66*	*2.0*	*5*	*2.08*	*6.4*	*6*	*2.99*	*11.6*				*0.15*[c]
1-CN[b]	1				5	2.09	4.8							1.33
	2	1	1.66	1.4	5	2.08	4.7							0.91
	3	1	1.66	1.3	4	2.08	3.1							0.87
	4	1	1.66	1.4	5	2.08	4.7	4	2.95	4.4				0.74
	5	**1**	**1.66**	**1.3**	**4**	**2.08**	**3.1**	**4**	**2.95**	**4.4**				**0.63**
	6	*1*	*1.66*	*1.7*	*4*	*2.08*	*3.3*	*4*	*2.95*	*4.8*				*0.69*[c]
1-OH[d]					6	2.05	7.5							2.08
		1	1.68	1.6	5	2.09	6.4							1.16
		1	1.68	1.3	4	2.10	4.5							1.04
		1	1.68	3.3	4	2.08	1.7				1[f]	1.94	-1.3	0.79
		1	1.68	1.4	4	2.10	4.4	6	3.06	5.0				0.54
		1	**1.68**	**2.4**	**4**	**2.10**	**2.1**	**6**	**3.03**	**6.2**	**1**[f]	**1.95**	**0.0**	**0.39**
		1	*1.69*	*2.4*	*4*	*2.09*	*1.8*	*6*	*3.02*	*6.4*	*1*[f]	*1.94*	*-0.8*	*0.20*[c]

[a]Fourier-transform range as follows: **1**-O_2CCF_3, and **1**-CN: 2 – 15 $Å^{-1}$ (resolution 0.12 Å); **1**-NCO, **1**-NCS, **1**-N_3, and **1**-OH: k = 2 – 14.5 $Å^{-1}$ (resolution 0.126 Å). Back-transformation ranges as follows: **1**-O_2CCF_3: R' = 0.60 – 3.20 Å; **1**-NCO: R' = 0.90 – 3.10 Å; **1**-NCS: R' = 0.90 – 5.00; **1**-N_3: R' = 0.92 – 3.00 Å; **1**-CN: R' = 0.60 – 3.20 Å; **1**-OH: R' = 0.90 – 3.10 Å. σ^2 is in units of 10^3 $Å^2$. [b]EXAFS data fit using the program SSEXAFS. [c]Fits to unfiltered data corresponding to best fits to filtered data. [d]EXAFS data fit using the program EXAFSPAK in conjunction with FEFF 6. [e]Includes four multiple scattering pathways involving two of the three atoms of the NCS^- ligand. [f]X = O.

Table S3. EXAFS fitting results for $[Fe^{IV}(O)(TMC)(OH)]^+$ (**1**-OH) with σ^2(Fe–OH) varied from 0.003 to -0.003 Å^2 in 0.0005 Å^2 increments and fixed during the fitting procedure.

	Fe–O			Fe–N			Fe–O			Fe–C			
fit	*n*	*r*(Å)	σ^2 (Å^2)	*n*	*r*(Å)	σ^2 (Å^2)	*n*	*r*(Å)	σ^2 (Å^2)	n	r(Å)	σ^2 (Å^2)	*F*
1	1	1.68	1.1	4	2.10	2.8	1	1.94	3.0	6	3.03	5.8	0.21
2	1	1.68	1.1	4	2.10	2.7	1	1.94	2.5	6	3.03	5.8	0.21
3	**1**	**1.68**	**1.2**	**4**	**2.10**	**2.6**	**1**	**1.94**	**2.0**	**6**	**3.03**	**5.9**	**0.21**
4	1	1.68	1.3	4	2.10	2.5	1	1.94	1.5	6	3.03	6.0	0.20
5	1	1.68	1.5	4	2.10	2.4	1	1.94	1.0	6	3.03	6.1	0.20
6	1	1.68	1.6	4	2.10	2.3	1	1.94	0.5	6	3.02	6.1	0.20
7	1	1.69	1.9	4	2.10	2.1	1	1.94	0.0	6	3.02	6.2	0.20
8	1	1.69	2.2	4	2.09	1.9	1	1.94	-0.5	6	3.02	6.3	0.20
9	1	1.69	2.5	4	2.09	1.7	1	1.94	-1.0	6	3.02	6.4	0.20
10	1	1.69	2.9	4	2.09	1.5	1	1.94	-1.5	6	3.01	6.5	0.20
11	1	1.69	3.4	4	2.09	1.2	1	1.94	-2.0	6	3.01	6.7	0.21
12	1	1.69	4.1	4	2.09	0.9	1	1.94	-2.5	6	3.00	6.8	0.21
13	1	1.70	4.8	4	2.08	0.6	1	1.94	-3.0	6	2.99	6.9	0.23

Table S4. Cartesian coordinates (Å) for DFT energy minimized model of $[Fe^{IV}(O)(TMC)(NCMe)]^{2+}$.

	x	y	z
Fe	0.000000	0.000000	0.000000
O	0.000000	0.000000	1.645981
N	0.083176	-2.116913	0.139923
N	2.154572	-0.099625	-0.012375
N	0.000000	2.156876	-0.012375
N	-2.110779	0.180908	0.139938
C	1.399017	-2.338226	0.835709
C	2.502533	-1.561417	0.160370
C	2.628143	0.688600	1.189392
C	2.286011	2.182724	1.168640
C	0.809265	2.593521	1.189407
C	-1.444122	2.571960	0.160385
C	-2.271072	1.505508	0.835739
C	-2.739182	-0.855545	1.034668
C	-2.417450	-2.308243	0.695190
C	-0.981140	-2.696793	1.034607
C	0.059600	-2.854126	-1.162094
C	2.922729	0.352707	-1.214188
C	0.487350	2.903305	-1.214172
C	-2.848297	0.191391	-1.162064
H	1.642746	-3.413208	0.837555
H	1.269760	-2.012680	1.873077
H	3.436996	-1.652969	0.735092
H	2.703339	-1.970383	-0.837692
H	2.195800	0.214691	2.077500
H	3.725433	0.582764	1.237350
H	2.726105	2.602905	2.086900
H	2.819397	2.692000	0.352875
H	0.754227	3.694534	1.237396
H	0.315948	2.183472	2.077530
H	-1.492400	3.509644	0.735153
H	-1.843400	2.791473	-0.837631
H	-3.333633	1.798691	0.837631
H	-1.951828	1.361313	1.873138
H	-2.394852	-0.642120	2.053940
H	-3.829254	-0.694138	1.004181
H	-3.065094	-2.926636	1.336990
H	-2.697784	-2.575928	-0.335205
H	-0.870270	-3.793137	1.004166
H	-0.752014	-2.362686	2.053925
H	0.190918	-3.931900	-0.978867
H	-0.900238	-2.696091	-1.664093
H	0.860611	-2.506134	-1.820023
H	3.993729	0.149628	-1.058075
H	2.587128	-0.193527	-2.099945
H	2.802307	1.422684	-1.385803
H	0.333939	3.982544	-1.058060
H	1.550659	2.733551	-1.385818
H	-0.073837	2.593323	-2.099930
H	-3.918854	0.372360	-0.978836
H	-2.463700	0.975479	-1.819962
H	-2.734787	-0.774750	-1.664093
N	-0.028290	-0.027023	-2.086472
C	-0.029617	-0.028244	-3.249207
C	-0.026398	-0.025208	-4.700500
H	-1.015656	0.267258	-5.080139
H	0.722794	0.690140	-5.073914
H	0.220032	-1.026886	-5.080124

Table S5. Cartesian coordinates (Å) for DFT energy minimized model of $[Fe^{IV}(O)(TMC)(O_2CCF_3)]^+$.

	x	y	z
Fe	0.000000	0.000000	0.000000
O	0.000000	0.000000	1.661362
N	0.094833	-2.123764	0.159775
N	2.153870	-0.089157	0.016678
N	0.000000	2.155716	0.016678
N	-2.117996	0.182510	0.159836
C	1.403107	-2.326584	0.865051
C	2.501373	-1.546982	0.182602
C	2.613312	0.683517	1.227341
C	2.270020	2.177963	1.218613
C	0.791031	2.582764	1.227371
C	-1.442169	2.563202	0.182678
C	-2.266510	1.498032	0.865173
C	-2.734528	-0.860641	1.045044
C	-2.403137	-2.305740	0.684860
C	-0.972916	-2.696625	1.045044
C	0.091217	-2.861984	-1.138016
C	2.931564	0.371185	-1.175232
C	0.492065	2.913727	-1.175232
C	-2.855789	0.209534	-1.137970
H	1.657990	-3.399704	0.879395
H	1.267212	-1.985535	1.896790
H	3.442368	-1.640274	0.748154
H	2.688568	-1.951202	-0.819443
H	2.168091	0.204880	2.106476
H	3.711411	0.579651	1.285202
H	2.701080	2.591553	2.144379
H	2.805145	2.691406	0.407227
H	0.732666	3.684235	1.285263
H	0.294403	2.157700	2.106506
H	-1.496506	3.507202	0.748306
H	-1.838379	2.766998	-0.819351
H	-3.328262	1.797119	0.879517
H	-1.931351	1.348175	1.896881
H	-2.381516	-0.660919	2.064377
H	-3.826920	-0.707367	1.024185
H	-3.066559	-2.942261	1.292100
H	-2.648682	-2.541336	-0.361847
H	-0.864990	-3.794418	1.024109
H	-0.758789	-2.352219	2.064362
H	0.242508	-3.936676	-0.945343
H	-0.859589	-2.710770	-1.653717
H	0.879500	-2.491913	-1.796555
H	3.999588	0.152328	-1.011673
H	2.581390	-0.138367	-2.074463
H	2.815200	1.441818	-1.337265
H	0.317612	3.989868	-1.011566
H	1.556976	2.753174	-1.337250
H	-0.031570	2.584961	-2.074402
H	-3.923294	0.405090	-0.945267
H	-2.453415	0.981827	-1.796448
H	-2.744049	-0.746719	-1.653717
O	-0.202300	-0.194107	-1.984650
C	0.184753	0.177322	-3.168030
O	1.033905	0.992065	-3.509949
C	-0.606461	-0.581802	-4.303940
F	-0.211411	-0.202713	-5.529816
F	-0.427948	-1.938690	-4.206772
F	-1.954849	-0.347290	-4.206787

Table S6. Cartesian coordinates (Å) for DFT energy minimized model of $[Fe^{IV}(O)(TMC)(NCO)]^{+}$.

	x	y	z
Fe	0.000000	0.000000	0.000000
O	0.000000	0.000015	1.673965
N	0.000000	-0.045929	-1.939545
C	0.000000	0.025421	-3.140778
O	0.000015	0.094925	-4.337296
N	1.587784	-1.404724	0.143585
N	1.553131	1.492340	0.003128
N	-1.553146	1.492355	0.003128
N	-1.587800	-1.404724	0.143585
C	2.646805	-0.604141	0.841583
C	2.843613	0.729919	0.161041
C	1.318146	2.369598	1.203827
C	0.000000	3.155823	1.189774
C	-1.318176	2.369583	1.203827
C	-2.843628	0.729935	0.161011
C	-2.646805	-0.604156	0.841553
C	-1.271240	-2.573456	1.030243
C	0.000015	-3.335449	0.673400
C	1.271225	-2.573471	1.030243
C	2.100464	-1.915573	-1.162170
C	1.743149	2.346924	-1.207397
C	-1.743118	2.346939	-1.207428
C	-2.100449	-1.915558	-1.162200
H	3.597336	-1.164413	0.850082
H	2.309708	-0.465912	1.874298
H	3.569611	1.339767	0.722321
H	3.257309	0.583420	-0.843903
H	1.350372	1.719788	2.085495
H	2.153366	3.090668	1.259735
H	-0.000015	3.759033	2.111633
H	-0.000015	3.894547	0.375092
H	-2.153397	3.090668	1.259705
H	-1.350388	1.719757	2.085495
H	-3.569641	1.339752	0.722290
H	-3.257324	0.583420	-0.843933
H	-3.597351	-1.164413	0.850052
H	-2.309723	-0.465897	1.874268
H	-1.172226	-2.178925	2.049011
H	-2.140152	-3.253281	1.005951
H	0.000015	-4.256226	1.277008
H	0.000015	-3.673157	-0.373352
H	2.140152	-3.253296	1.005981
H	1.172241	-2.178940	2.049011
H	2.981461	-2.554703	-0.986740
H	1.323181	-2.496460	-1.666260
H	2.366135	-1.087372	-1.822403
H	2.660797	2.945831	-1.089706
H	1.824310	1.712769	-2.093658
H	0.905243	3.030090	-1.345900
H	-2.660812	2.945862	-1.089737
H	-0.905243	3.030075	-1.345900
H	-1.824295	1.712769	-2.093689
H	-2.981476	-2.554703	-0.986771
H	-2.366135	-1.087372	-1.822433
H	-1.323151	-2.496475	-1.666260

Table S7. Cartesian coordinates (Å) for DFT energy minimized model of $[Fe^{IV}(O)(TMC)(NCS)]^{+}$.

	x	y	z
Fe	0.000000	0.000000	0.000000
O	0.000000	0.000000	1.676468
N	-0.026886	-0.025711	-1.931091
C	-0.061798	-0.059113	-3.128632
S	-0.127029	-0.121536	-4.734833
N	0.080353	-2.117172	0.137405
N	2.149612	-0.095551	-0.005402
N	0.000000	2.151749	-0.005417
N	-2.111481	0.174240	0.137390
C	1.389404	-2.332489	0.837173
C	2.491608	-1.554672	0.157364
C	2.625702	0.686874	1.189087
C	2.281876	2.182724	1.168427
C	0.802765	2.592636	1.189102
C	-1.442535	2.558182	0.157333
C	-2.268509	1.491562	0.837143
C	-2.740875	-0.864243	1.019623
C	-2.412766	-2.307907	0.658112
C	-0.985092	-2.699783	1.019623
C	0.067871	-2.835907	-1.171875
C	2.891418	0.352737	-1.223267
C	0.480743	2.872910	-1.223267
C	-2.830093	0.193695	-1.171875
H	1.638977	-3.407196	0.845718
H	1.255402	-1.992798	1.869629
H	3.432800	-1.655746	0.721207
H	2.674591	-1.958008	-0.845886
H	2.182739	0.218613	2.075409
H	3.724365	0.582900	1.240860
H	2.723953	2.605606	2.084610
H	2.810196	2.688095	0.346848
H	0.747696	3.694839	1.240860
H	0.315308	2.170883	2.075394
H	-1.501724	3.502930	0.721176
H	-1.837341	2.758865	-0.845947
H	-3.331100	1.788635	0.845688
H	-1.935089	1.342621	1.869598
H	-2.389023	-0.666565	2.039734
H	-3.832336	-0.704224	0.993195
H	-3.081207	-2.947327	1.255112
H	-2.651398	-2.536194	-0.390915
H	-0.873657	-3.797302	0.993195
H	-0.771927	-2.357071	2.039703
H	0.214828	-3.914993	-1.000931
H	-0.888748	-2.675705	-1.677277
H	0.851028	-2.455338	-1.831100
H	3.958984	0.103378	-1.110718
H	2.484573	-0.145981	-2.106766
H	2.805800	1.430100	-1.365051
H	0.279022	3.950485	-1.110764
H	1.553253	2.739532	-1.365036
H	-0.035507	2.488571	-2.106766
H	-3.901581	0.388428	-1.000931
H	-2.415131	0.959183	-1.831161
H	-2.712509	-0.769104	-1.677277

Table S8. Cartesian coordinates (Å) for DFT energy minimized model of $[Fe^{IV}(O)(TMC)(N_3)]^+$.

	x	y	z
Fe	0.000107	0.000000	0.000000
O	0.000107	0.000031	1.676346
N	-0.061630	-0.059387	-1.928040
N	0.025864	0.024765	-3.122665
N	0.094604	0.090866	-4.287140
N	0.088684	-2.118622	0.147018
N	2.150848	-0.083740	0.006226
N	0.000107	2.152390	0.006180
N	-2.113495	0.170959	0.147003
C	1.402588	-2.328842	0.838608
C	2.498398	-1.542358	0.158279
C	2.618958	0.689743	1.210052
C	2.271851	2.185013	1.200241
C	0.791229	2.590042	1.210022
C	-1.443909	2.556427	0.158218
C	-2.272415	1.492050	0.838593
C	-2.733643	-0.864151	1.038345
C	-2.402573	-2.310913	0.688660
C	-0.969788	-2.698074	1.038330
C	0.068832	-2.839111	-1.160416
C	2.895813	0.377075	-1.203796
C	0.489609	2.878845	-1.203812
C	-2.834167	0.179123	-1.160461
H	1.658905	-3.402039	0.842560
H	1.271912	-1.993103	1.872665
H	3.442169	-1.643433	0.718018
H	2.679688	-1.938751	-0.848145
H	2.168961	0.213547	2.088226
H	3.717392	0.586472	1.268661
H	2.702621	2.599319	2.125732
H	2.808000	2.700668	0.390121
H	0.730804	3.691666	1.268616
H	0.297852	2.158920	2.088196
H	-1.508133	3.503433	0.717987
H	-1.832886	2.752960	-0.848236
H	-3.334793	1.789932	0.842514
H	-1.942000	1.348465	1.872604
H	-2.377151	-0.657074	2.054733
H	-3.826263	-0.710159	1.016632
H	-3.060669	-2.943878	1.304200
H	-2.656265	-2.554932	-0.353363
H	-0.858444	-3.795822	1.016693
H	-0.749054	-2.349838	2.054764
H	0.210358	-3.918976	-0.988815
H	-0.887863	-2.673477	-1.663712
H	0.854111	-2.463531	-1.820313
H	3.965164	0.135712	-1.088593
H	2.501038	-0.121918	-2.092758
H	2.804657	1.454544	-1.340057
H	0.290054	3.956726	-1.088623
H	1.562698	2.745804	-1.340103
H	-0.024338	2.503738	-2.092819
H	-3.907715	0.362595	-0.988831
H	-2.428329	0.949188	-1.820343
H	-2.705856	-0.783264	-1.663742

Table S9. Cartesian coordinates (Å) for DFT energy minimized model of $[Fe^{IV}(O)(TMCS)]^{+}$.

	x	y	z
Fe	0.002703	-0.020720	0.016341
O	0.001159	-0.009457	-1.680742
N	-0.003311	2.152518	-0.153076
N	2.127517	0.182007	0.064928
N	0.119818	-2.190763	-0.031106
N	-2.087668	-0.256204	-0.089769
C	1.317946	2.381915	-0.822151
C	2.417615	1.657070	-0.078910
C	2.669117	-0.553382	-1.136481
C	2.395853	-2.064132	-1.184446
C	0.938358	-2.549825	-1.245172
C	-1.309578	-2.643504	-0.179305
C	-2.214132	-1.588023	-0.777340
C	-2.783459	0.737418	-0.987709
C	-2.486271	2.212847	-0.712006
C	-1.070275	2.636429	-1.093761
C	-0.075596	2.950861	1.108203
C	2.857896	-0.253822	1.292742
C	0.642403	-2.942730	1.151979
C	-2.776122	-0.201829	1.260902
S	-0.239688	-0.013576	2.345848
C	-1.946508	-0.692646	2.435524
H	1.538147	3.463490	-0.864443
H	1.231367	2.003477	-1.846373
H	2.525189	2.068529	0.932017
H	3.385411	1.795751	-0.588038
H	3.763346	-0.397436	-1.146772
H	2.234014	-0.077008	-2.022612
H	2.879462	-2.423005	-2.108027
H	2.940232	-2.572753	-0.374940
H	0.440349	-2.114384	-2.118926
H	0.937131	-3.651158	-1.336293
H	-1.346039	-3.554924	-0.798912
H	-1.666245	-2.921130	0.818768
H	-3.259836	-1.938994	-0.742698
H	-1.937667	-1.409488	-1.822676
H	-3.868411	0.550508	-0.908700
H	-2.468230	0.507896	-2.012110
H	-2.724858	2.498542	0.323791
H	-3.182867	2.794852	-1.336270
H	-0.829307	2.225339	-2.081317
H	-1.003417	3.737563	-1.143059
H	0.029581	4.024549	0.872245
H	0.702508	2.651464	1.815262
H	-1.025996	2.773808	1.618569
H	3.923805	0.014730	1.206271
H	2.776821	-1.331144	1.434951
H	2.425947	0.237808	2.170293
H	0.427051	-4.016484	1.029494
H	0.168515	-2.555687	2.059923
H	1.721578	-2.824711	1.260709
H	-3.735157	-0.747204	1.182064
H	-3.011631	0.853574	1.437831
H	-2.409571	-0.334878	3.365577
H	-1.918326	-1.789472	2.501966

Table S10. Cartesian coordinates (Å) for DFT energy minimized model of $[Fe^{IV}(O)(TMC)(CN)]^{+}$.

	x	y	z
Fe	0.000000	0.000000	0.000000
O	0.000000	0.000015	1.684189
C	-0.044937	-0.042847	-2.011292
N	-0.059280	-0.056625	-3.184464
N	0.072174	-2.121796	0.128342
N	2.140900	-0.098892	-0.025223
N	-0.000015	2.143188	-0.025238
N	-2.116226	0.169998	0.128357
C	1.384430	-2.334122	0.823914
C	2.482010	-1.558716	0.135513
C	2.623000	0.681870	1.170227
C	2.280700	2.177811	1.153152
C	0.802155	2.588745	1.170242
C	-1.442566	2.551270	0.135544
C	-2.267776	1.490616	0.823959
C	-2.742188	-0.864243	1.017807
C	-2.417862	-2.308792	0.658249
C	-0.989853	-2.699417	1.017822
C	0.056198	-2.858612	-1.173645
C	2.890350	0.350540	-1.241455
C	0.483505	2.871063	-1.241455
C	-2.852982	0.188049	-1.173645
H	1.634338	-3.408661	0.834579
H	1.255920	-1.991974	1.856613
H	3.427246	-1.658661	0.692627
H	2.656600	-1.961578	-0.869202
H	2.185455	0.212189	2.058578
H	3.721802	0.577209	1.215149
H	2.720612	2.597870	2.071686
H	2.811447	2.684600	0.334305
H	0.748337	3.691193	1.215179
H	0.312790	2.173325	2.058594
H	-1.498749	3.500107	0.692657
H	-1.836945	2.744308	-0.869186
H	-3.329620	1.789871	0.834595
H	-1.931885	1.346481	1.856628
H	-2.385803	-0.664474	2.036011
H	-3.833420	-0.702316	0.995483
H	-3.086197	-2.946915	1.256531
H	-2.657028	-2.537125	-0.390442
H	-0.878433	-3.796967	0.995468
H	-0.773834	-2.352600	2.035995
H	0.207886	-3.934692	-0.987854
H	-0.902237	-2.706100	-1.677628
H	0.831787	-2.481384	-1.843903
H	3.954575	0.088516	-1.126419
H	2.475204	-0.132858	-2.130325
H	2.817230	1.430283	-1.372757
H	0.270874	3.946274	-1.126419
H	1.558716	2.748276	-1.372742
H	-0.018555	2.478683	-2.130310
H	-3.920929	0.389191	-0.987823
H	-2.440384	0.945389	-1.843872
H	-2.744873	-0.776398	-1.677597

Table S11. Cartesian coordinates (Å) for DFT energy minimized model of $[Fe^{IV}(O)(TMC)(OH)]^{+}$.

	x	y	z
Fe	-0.000046	-0.000015	0.000000
O	-0.000046	0.000000	1.691620
O	-0.070770	-0.067780	-1.892532
H	0.549240	0.526276	-2.347733
N	0.076431	-2.103455	0.119995
N	2.155914	-0.092072	-0.006577
N	-0.000061	2.157928	-0.006607
N	-2.098328	0.166138	0.119995
C	1.384171	-2.332642	0.816635
C	2.494690	-1.552551	0.153687
C	2.623474	0.687866	1.192596
C	2.279282	2.184067	1.171448
C	0.799133	2.591782	1.192596
C	-1.444748	2.558685	0.153641
C	-2.271500	1.482437	0.816605
C	-2.742676	-0.865875	0.996780
C	-2.417236	-2.316193	0.651917
C	-0.982117	-2.703186	0.996826
C	0.057632	-2.785110	-1.208084
C	2.903061	0.354248	-1.217545
C	0.477783	2.885315	-1.217575
C	-2.780106	0.176407	-1.208130
H	1.629913	-3.408752	0.811951
H	1.247910	-2.002686	1.852005
H	3.428970	-1.657852	0.728775
H	2.688034	-1.953369	-0.848938
H	2.162933	0.220016	2.070358
H	3.721695	0.581741	1.259735
H	2.718826	2.605255	2.089859
H	2.810547	2.693146	0.353317
H	0.739944	3.693481	1.259689
H	0.312042	2.151627	2.070328
H	-1.510086	3.496582	0.728729
H	-1.836900	2.768936	-0.848984
H	-3.336151	1.773834	0.811935
H	-1.947662	1.332275	1.851974
H	-2.402084	-0.662018	2.019836
H	-3.833817	-0.704361	0.955750
H	-3.072586	-2.944183	1.276413
H	-2.677643	-2.565750	-0.387833
H	-0.867310	-3.800262	0.955780
H	-0.763916	-2.371613	2.019867
H	0.227066	-3.865829	-1.070663
H	-0.909073	-2.622849	-1.692780
H	0.812119	-2.354400	-1.869110
H	3.973969	0.118729	-1.101868
H	2.514160	-0.167786	-2.098114
H	2.812119	1.431229	-1.369080
H	0.288162	3.965286	-1.101883
H	1.549896	2.748489	-1.369080
H	-0.060394	2.519028	-2.098160
H	-3.852615	0.391785	-1.070694
H	-2.317612	0.911835	-1.869156
H	-2.659256	-0.796326	-1.692810

Table S12. Mulliken spin densities and compositions of spin-down molecular orbitals involved in Fe=O bonding based on BP86 DFT computations for $[Fe^{IV}(O)(TMC)(X)]^{2+/+}$ (**1**-X) complexes.

	Spin density		Fe d_{xz} MO (β)			Fe d_{yz} MO (β)			Fe d_z^2 MO (β)		
	Fe	O	Fe 3d	O 2p	X 2p	Fe 3d	O 2p	X 2p	Fe 3d	O 2p	X 2p
1-NCMe	1.31	0.77	53	37	4	53	37	4	54	22	3
1-O_2CCF_3	1.38	0.70	58	34	<1	60	34	<1	54	20	2
1-NCO	1.32	0.69	56	33	4	57	33	4	53	18	1
1-NCS	1.27	0.69	53	33	8	54	33	8	53	18	2
1-N_3	1.26	0.65	53	31	11	54	32	10	53	19	3
1′-SR	1.32	0.70	56	36	<1	56	30	9	50	17	11
1-CN	1.32	0.76	55	36	4	55	36	4	51	17	2
1-OH	1.35	0.67	59	35	<1	58	30	8	52	16	6

Table S13. TD-DFT Calculated Energies (cm^{-1}), Percent Contributions from Dominant One-electron Excitations, and Oscillator Strengths for the Major Electronic Transitions of $[Fe^{IV}(O)(TMC)(NCMe)]^{2+}$ (**1**-NCMe) Using the BP86, B3LYP, and PBE0 Functionals.

band	state	energy (cm^{-1})[a]	f_{osc}	transition[b]	%	donor MO	acceptor MO	comments
BP86								
	1	10 900	0.00002	97β → 98β	91	Fe d_{xy}	Fe d_{yz}	Fe^{IV} d → d
	2	11 500	0.00002	97β → 99β	91	Fe d_{xy}	Fe d_{xz}	Fe^{IV} d → d
	3	12 900	0.00001	97β → 100β	56	Fe d_{xy}	Fe $d_{x^2-y^2}$	Fe^{IV} d → d
				97α → 100α	43	Fe d_{xy}	Fe $d_{x^2-y^2}$	Fe^{IV} d → d
i	4	14 300	0.00284	99α → 100α	88	Fe d_{xz}	Fe $d_{x^2-y^2}$	Fe^{IV} d → d
	5	14 800	0.00323	98α → 100α	87	Fe d_{yz}	Fe $d_{x^2-y^2}$	Fe^{IV} d → d
ii	13	26 100	0.00621	96β → 98β	36	O p_y	Fe d_{yz}	O^{2-} → Fe^{IV} CT
				94β → 98β	32	O p_y	Fe d_{yz}	O^{2-} → Fe^{IV} CT
				95β → 99β	21	O p_x	Fe d_{xz}	O^{2-} → Fe^{IV} CT
	14	26 900	0.02117	96α → 100α	68	N_{TMC} p	Fe $d_{x^2-y^2}$	N_{TMC} → Fe^{IV} CT
				96β → 100β	22	O p_y	Fe $d_{x^2-y^2}$	O^{2-} → Fe^{IV} CT
	15	28 000	0.01098	95α → 100α	48	N_{TMC} p	Fe $d_{x^2-y^2}$	N_{TMC} → Fe^{IV} CT
				95β → 100β	23	O p_x	Fe $d_{x^2-y^2}$	O^{2-} → Fe^{IV} CT
				94β → 99β	14	O p_y	Fe d_{xz}	O^{2-} → Fe^{IV} CT
B3LYP								
	1	11 700	<0.00001	97β → 100β	58	Fe d_{xy}	Fe $d_{x^2-y^2}$	Fe^{IV} d → d
				95α → 100α	36	Fe d_{xy}	Fe $d_{x^2-y^2}$	Fe^{IV} d → d
	2	12 600	<0.00001	97β → 98β	86	Fe d_{xy}	Fe d_{yz}	Fe^{IV} d → d
	3	12 700	<0.00001	97β → 99β	88	Fe d_{xy}	Fe d_{xz}	Fe^{IV} d → d
i	4	16 700	0.00310	99α → 100α	61	Fe d_{xz}	Fe $d_{x^2-y^2}$	Fe^{IV} d → d
	5	17 000	0.00320	98α → 100α	54	Fe d_{yz}	Fe $d_{x^2-y^2}$	Fe^{IV} d → d
ii	13	27 400	0.01532	96β → 98β	32	O p_y	Fe d_{yz}	O^{2-} → Fe^{IV} CT
				95β → 99β	28	O p_x	Fe d_{xz}	O^{2-} → Fe^{IV} CT
iii	14	29 300	0.00956	96β → 100β	37	O p_y	Fe $d_{x^2-y^2}$	O^{2-} → Fe^{IV} CT
				95β → 101β	15	O p_x	Fe d_{z^2}	O^{2-} → Fe^{IV} CT
PBE0								
	1	9 700	<0.00001	95β → 100β	58	Fe d_{xy}	Fe $d_{x^2-y^2}$	Fe^{IV} d → d
				95α → 100α	32	Fe d_{xy}	Fe $d_{x^2-y^2}$	Fe^{IV} d → d
	2	12 700	0.00001	95β → 99β	82	Fe d_{xy}	Fe d_{xz}	Fe^{IV} d → d
	3	12 700	0.00001	95β → 98β	81	Fe d_{xy}	Fe d_{yz}	Fe^{IV} d → d
i	4	16 200	0.00251	99α → 100α	42	Fe d_{xz}	Fe $d_{x^2-y^2}$	Fe^{IV} d → d
	5	16 500	0.00325	98α → 100α	45	Fe d_{yz}	Fe $d_{x^2-y^2}$	Fe^{IV} d → d
				97α → 100α	20	N_{TMC} $p_{x/y}$	Fe $d_{x^2-y^2}$	Fe^{IV} d → d
ii	13	26 700	0.01625	97β → 99β	28	O p_x	Fe d_{xz}	O^{2-} → Fe^{IV} CT
				96β → 98β	26	O p_y	Fe d_{yz}	O^{2-} → Fe^{IV} CT
				96α → 100α	19	N_{TMC} $p_{x/y}$	Fe $d_{x^2-y^2}$	N_{TMC} → Fe^{IV} CT
	14	28 900	0.00676	96β → 100β	38	O p_y	Fe $d_{x^2-y^2}$	O^{2-} → Fe^{IV} CT
				97β → 101β	26	O p_x	Fe d_{z^2}	O^{2-} → Fe^{IV} CT
				98α → 100α	15	Fe d_{yz}	Fe $d_{x^2-y^2}$	Fe^{IV} d → d
	15	29 100	0.00163	97β → 100β	37	O p_x	Fe $d_{x^2-y^2}$	O^{2-} → Fe^{IV} CT
				96β → 101β	31	O p_y	Fe d_{z^2}	O^{2-} → Fe^{IV} CT
	16	30 900	0.01145	97β → 101β	35	O p_x	Fe d_{z^2}	O^{2-} → Fe^{IV} CT

[a]Energies have been rounded to the nearest 100 cm^{-1}. [b]Compositions of molecular orbitals (MOs) involved in these electronic transitions are listed in Tables S14 – S16. Spin-up and spin-down MOs are designated by α and β, respectively.

Table S14. Energies (eV) and Compositions (%) of the Fe 3d-, O 2p-, and N 2p-Based MOs from Spin-Unrestricted B3LYP DFT Computations Performed on a Model of $[Fe^{IV}(O)(TMC)(NCMe)]^{2+}$.

orbital	description	occup	spin	energy	Fe 3d	Fe 4p	O 2p	N_{axial} 2p	N_{TMC} 2p[a]
95α	Fe d_{xy}	1.0	↑	-15.46	84.6	0	0.2	0	3.9
97α	N_{TMC} 2p	1.0	↑	-14.52	14.5	6.5	13.9	0	26.5
98α	Fe d_{yz}	1.0	↑	-13.72	22.9	0.7	39.6	0	19.6
99α	Fe d_{xz}	1.0	↑	-13.70	26.3	0.2	45.0	0.1	14.7
100α	Fe $d_{x^2-y^2}$	0.0	↑	-9.24	61.5	0	0	0	25.2
101α	Fe d_{z^2}	0.0	↑	-8.46	56.5	1.7	20.2	1.4	9.8
95β	O p_x	1.0	↓	-14.12	34.7	0.6	32.7	15.4	0
96β	O p_y	1.0	↓	-14.10	26.4	1.9	22.6	0.2	25.1
97β	Fe d_{xy}	1.0	↓	-14.00	92.0	0	0.6	0	2.0
98β	Fe d_{yz}	0.0	↓	-9.33	51.4	0.7	37.2	0.7	1.3
99β	Fe d_{xz}	0.0	↓	-9.25	52.8	0.9	35.8	0.8	1.3
100β	Fe $d_{x^2-y^2}$	0.0	↓	-8.17	71.4	0	0	17.9	0
101β	Fe d_{z^2}	0.0	↓	-7.72	59.1	1.9	18.9	1.1	8.2

[a]Sum of contributions from the four nitrogen atoms of the TMC macrocycle.

Table S15. Energies (eV) and Compositions (%) of the Fe 3d-, O 2p-, and N 2p-Based MOs from Spin-Unrestricted BP86 DFT Computations Performed on a Model of $[Fe^{IV}(O)(TMC)(NCMe)]^{2+}$.

orbital	description	occup	spin	energy	Fe 3d	Fe 4p	O 2p	N_{axial} 2p	N_{TMC} 2p[a]
95α	N_{TMC} 2p	1.0	↑	-13.57	6.6	6.3	0	0	50.0
96α	N_{TMC} 2p	1.0	↑	-13.36	5.9	6.2	0.2	0	42.4
97α	Fe d_{xy}	1.0	↑	-12.30	94.9	0	0	0	1.2
98α	Fe d_{yz}	1.0	↑	-11.84	46.7	0.2	41.2	0	4.2
99α	Fe d_{xz}	1.0	↑	-11.77	47.2	0.2	41.9	0	4.0
100α	Fe $d_{x^2-y^2}$	0.0	↑	-10.00	57.5	0	0	0	27.8
101α	Fe d_{z^2}	0.0	↑	-9.24	54.2	1.8	21.7	1.5	10.8
94β	O p_y	1.0	↓	-13.62	16.5	4.2	29.1	0	16.6
95β	O p_x	1.0	↓	-13.16	31.1	0.8	31.3	0	18.4
96β	O p_y + Fe d_{yz}	1.0	↓	-13.14	22.2	2.2	18.9	0.2	29.2
97β	Fe d_{xy}	1.0	↓	-11.59	95.1	0	0	0	0.8
98β	Fe d_{yz}	0.0	↓	-10.13	53.7	0.4	36.0	0.5	1.4
99β	Fe d_{xz}	0.0	↓	-10.05	54.4	0.6	35.3	0.6	1.8
100β	Fe $d_{x^2-y^2}$	0.0	↓	-9.28	67.0	0	0	0	21.0
101β	Fe d_{z^2}	0.0	↓	-8.66	56.5	1.6	21	1.2	9.0

[a]Sum of contributions from the four nitrogen atoms of the TMC macrocycle.

Table S16. Energies (eV) and Compositions (%) of the Fe 3d-, O 2p-, N 2p-Based MOs from Spin-Unrestricted PBE0 DFT Computations Performed on a Model of $[Fe^{IV}(O)(TMC)(NCMe)]^{2+}$.

orbital	description	occup	spin	energy	Fe 3d	Fe 4p	O 2p	N_{axial} 2p	N_{TMC} 2p[a]
95α	Fe d_{xy}	1.0	↑	-15.32	73.6	0	0.5	0	7.2
96α	N_{TMC} 2p	1.0	↑	-14.97	8.9	6.5	10.7	0.2	35.5
97α	N_{TMC} 2p	1.0	↑	-14.84	16.0	5.4	22.0	0.4	21.0
98α	Fe d_{yz}	1.0	↑	-14.06	16.2	1.3	34.8	0	25.5
99α	Fe d_{xz}	1.0	↑	-14.05	20.3	0.4	43.4	0	19.2
100α	Fe $d_{x^2-y^2}$	0.0	↑	-9.17	60.9	0	0	0	25.2
101α	Fe d_{z^2}	0.0	↑	-8.31	55.7	1.6	21.2	1.3	9.9
95β	Fe d_{xy}	1.0	↓	-14.46	91.9	0	0.5	0	2.3
96β	O p_y	1.0	↓	-14.29	29.0	1.2	27.6	0.2	21.3
97β	O p_x	1.0	↓	-14.28	32.7	0.4	36.1	0.2	14.2
98β	Fe d_{yz}	0.0	↓	-9.01	51.2	0.6	36.4	0.9	1.6
99β	Fe d_{xz}	0.0	↓	-8.91	53.2	0.8	34.2	1.1	1.4
100β	Fe $d_{x^2-y^2}$	0.0	↓	-7.87	72.8	0	0	0	16.4
101β	Fe d_{z^2}	0.0	↓	-7.47	59.3	1.7	19.1	1.1	7.8

[a]Sum of contributions from the four nitrogen atoms of the TMC macrocycle.

Table S17. TD-DFT Calculated Energies (cm^{-1}), Percent Contributions from Dominant One-electron Excitations, and Oscillator Strengths for the Major Electronic Transitions of $[Fe^{IV}(O)(TMC)(N_3)]^+$ (**1**-N_3) Using the PBE0 Functionals.

band	state	energy (cm^{-1})[a]	f_{osc}	transition[b]	%	donor MO	acceptor MO	comments
1-N_3								
iii	1	7 800	0.00001	93β → 100β	56	Fe d_{xy}	Fe $d_{x^2-y^2}$	Fe^{IV} d → d
				93α → 100α	34	Fe d_{xy}	Fe $d_{x^2-y^2}$	Fe^{IV} d → d
	2	10 600	0.00018	99α → 100α	46	N_3 p_y	Fe $d_{x^2-y^2}$	N_3 → Fe^{IV} CT
				97α → 100α	28	Fe d_{xz}	Fe $d_{x^2-y^2}$	Fe^{IV} d → d
	3	11 800	0.00029	96α → 100α	32	Fe d_{yz}	Fe $d_{x^2-y^2}$	Fe^{IV} d → d
				98α → 100α	25	N_3 $p_{x/z}$	Fe $d_{x^2-y^2}$	N_3 → Fe^{IV} CT
				93β → 99β	22	Fe d_{xy}	Fe d_{xz}	Fe^{IV} d → d
	4	14 000	0.00030	93β → 99β	65	Fe d_{xy}	Fe d_{xz}	Fe^{IV} d → d
	5	14 300	0.00018	93β → 98β	75	Fe d_{xy}	Fe d_{yz}	Fe^{IV} d → d
iv	11	19 600	0.00180	96α → 101α	30	Fe d_{yz}	Fe d_{z^2}	Fe^{IV} d → d
				98α → 101α	22	N_3 $p_{x/z}$	Fe d_{z^2}	N_3 → Fe^{IV} CT
	12	20 100	0.00422	98α → 100α	52	N_3 $p_{x/z}$	Fe $d_{x^2-y^2}$	N_3 → Fe^{IV} CT
				96α → 100α	28	Fe d_{yz}	Fe $d_{x^2-y^2}$	Fe^{IV} d → d
	14	20 600	0.00466	97α → 100α	32	Fe d_{xz}	Fe $d_{x^2-y^2}$	Fe^{IV} d → d
				99α → 100α	22	N_3 p_y	Fe $d_{x^2-y^2}$	N_3 → Fe^{IV} CT
v	15	22 800	0.01080	96β → 98β	54	N_3 $p_{x/z}$	Fe d_{yz}	N_3 → Fe^{IV} CT
				95β → 98β	13	O p_y	Fe d_{yz}	O → Fe^{IV} CT
	17	23 300	0.02010	97β → 99β	53	N_3 p_y	Fe d_{xz}	N_3 → Fe^{IV} CT
				95β → 98β	13	O p_y	Fe d_{yz}	O → Fe^{IV} CT
vi	23	27 600	0.01638	96β → 101β	37	N_3 $p_{x/z}$	Fe d_{z^2}	N_3 → Fe^{IV} CT
				98α → 101α	14	N_3 $p_{x/z}$	Fe d_{z^2}	N_3 → Fe^{IV} CT
	24	28 800	0.01589	95β → 101β	31	O p_y	Fe d_{z^2}	O → Fe^{IV} CT
				97β → 101β	15	N_3 p_y	Fe d_{z^2}	N_3 → Fe^{IV} CT
				98α → 101α	14	N_3 $p_{x/z}$	Fe d_{z^2}	N_3 → Fe^{IV} CT
	27	30 400	0.01475	94β → 100β	49	O p_x	Fe $d_{x^2-y^2}$	O → Fe^{IV} CT
				95β → 101β	13	O p_y	Fe d_{z^2}	O → Fe^{IV} CT
	28	31 700	0.06437	95α → 100α	53	N_{TMC} $p_{x/y}$	Fe $d_{x^2-y^2}$	N_{TMC} → Fe^{IV} CT
	32	33 100	0.05991	94α → 100α	53	N_{TMC} $p_{x/y}$	Fe $d_{x^2-y^2}$	N_{TMC} → Fe^{IV} CT
				94β → 100β	10	O p_x	Fe $d_{x^2-y^2}$	O → Fe^{IV} CT

[a]Energies have been rounded to the nearest 100 cm^{-1}. [b]Compositions of molecular orbitals (MOs) involved in these electronic transitions are listed in Tables S20. Spin-up and spin-down MOs are designated by α and β, respectively.

Table S18. TD-DFT Calculated Energies (cm^{-1}), Percent Contributions from Dominant One-electron Excitations, and Oscillator Strengths for the Major Electronic Transitions of $[Fe^{IV}(O)(TMC)(NCO)]^+$ (**1**-NCO) Using the PBE0 Functionals.

band	state	energy (cm^{-1})[a]	f_{osc}	transition	%	donor MO	acceptor MO	comments
1-NCO								
	1	8 100	<0.00001	93β → 100β	57	Fe d_{xy}	Fe $d_{x^2-y^2}$	Fe^{IV} d → d
				93α → 100α	32	Fe d_{xy}	Fe $d_{x^2-y^2}$	Fe^{IV} d → d
i	2	11 600	0.00046	98α → 100α	34	NCO p_y	Fe $d_{x^2-y^2}$	NCO → Fe^{IV} CT
				97α → 100α	23	Fe d_{xz}	Fe $d_{x^2-y^2}$	Fe^{IV} d → d
				93β → 98β	14	Fe d_{xy}	Fe d_{yz}	Fe^{IV} d → d
	3	11 700	0.00034	99α → 100α	31	NCO p_x	Fe $d_{x^2-y^2}$	NCO → Fe^{IV} CT
				96α → 100α	23	Fe d_{yz}	Fe $d_{x^2-y^2}$	Fe^{IV} d → d
				93β → 99β	18	Fe d_{xy}	Fe d_{xz}	Fe^{IV} d → d
	4	14 200	0.00034	93β → 99β	69	Fe d_{xy}	Fe d_{xz}	Fe^{IV} d → d
	5	14 600	0.00044	93β → 98β	72	Fe d_{xy}	Fe d_{yz}	Fe^{IV} d → d
	6	15 000	0.00006	93α → 100α	45	Fe d_{xy}	Fe $d_{x^2-y^2}$	Fe^{IV} d → d
				93β → 100β	36	Fe d_{xy}	Fe $d_{x^2-y^2}$	Fe^{IV} d → d
ii(sh)	13	24 000	0.01174	96α → 100α	50	Fe d_{yz}	Fe $d_{x^2-y^2}$	Fe^{IV} d → d
				99α → 100α	36	NCO p_x	Fe $d_{x^2-y^2}$	NCO → Fe^{IV} CT
	14	24 200	0.01017	97α → 100α	54	Fe d_{xz}	Fe $d_{x^2-y^2}$	Fe^{IV} d → d
				98α → 100α	34	NCO p_y	Fe $d_{x^2-y^2}$	NCO → Fe^{IV} CT
iii	15	26 300	0.04242	96β → 99β	18	NCO p_x	Fe d_{xz}	NCO → Fe^{IV} CT
				97β → 98β	17	NCO p_y	Fe d_{yz}	NCO → Fe^{IV} CT
				95β → 99β	14	O p_y	Fe d_{xz}	O → Fe^{IV} CT
				92α → 100α	13	N_{TMC} p	Fe $d_{x^2-y^2}$	N_{TMC} → Fe^{IV} CT
iv	22	30 200	0.05253	96β → 99β	24	NCO p_x	Fe d_{xz}	NCO → Fe^{IV} CT
				92α → 100α	16	N_{TMC} p	Fe $d_{x^2-y^2}$	N_{TMC} → Fe^{IV} CT
				97β → 98β	14	NCO p_y	Fe d_{yz}	NCO → Fe^{IV} CT
	23	30 500	0.01363	96β → 101β	23	NCO p_x	Fe d_{z^2}	NCO → Fe^{IV} CT
				95β → 101β	18	O p_y	Fe d_{z^2}	O → Fe^{IV} CT

[a]Energies have been rounded to the nearest 100 cm^{-1}.

Table S19. TD-DFT Calculated Energies (cm^{-1}), Percent Contributions from Dominant One-electron Excitations, and Oscillator Strengths for the Major Electronic Transitions of $[Fe^{IV}(O)(TMC)(NCS)]^+$ (**1**-NCS) Using the PBE0 Functionals.

band	state	energy (cm^{-1})[a]	f_{osc}	transition	%	donor MO	acceptor MO	comments
1-NCS								
	1	8 200	<0.00001	97β → 104β	57	Fe d_{xy}	Fe $d_{x^2-y^2}$	Fe^{IV} d → d
				97α → 104α	33	Fe d_{xy}	Fe $d_{x^2-y^2}$	Fe^{IV} d → d
i	2	11 200	0.00024	103α → 104α	38	NCS p_y	Fe $d_{x^2-y^2}$	NCS → Fe^{IV} CT
				101α → 104α	32	Fe d_{xz}	Fe $d_{x^2-y^2}$	Fe^{IV} d → d
				97β → 102β	10	Fe d_{xy}	Fe d_{yz}	Fe^{IV} d → d
	3	11 400	0.00016	102α → 104α	37	NCS p	Fe $d_{x^2-y^2}$	NCS → Fe^{IV} CT
				100α → 104α	29	Fe d_{yz}	Fe $d_{x^2-y^2}$	Fe^{IV} d → d
				97β → 103β	13	Fe d_{xy}	Fe d_{xz}	Fe^{IV} d → d
	4	13 900	0.0015	97β → 103β	75	Fe d_{xy}	Fe d_{xz}	Fe^{IV} d → d
	5	14 300	0.00015	97β → 102β	76	Fe d_{xy}	Fe d_{yz}	Fe^{IV} d → d
ii	7	16 300	0.00039	99β → 102β	29	O p_y	Fe d_{yz}	O → Fe^{IV} CT
				101β → 102β	21	NCS p_y	Fe d_{yz}	NCS → Fe^{IV} CT
				100β → 102β	19	NCS p_x	Fe d_{yz}	NCS → Fe^{IV} CT
	8	16 300	0.00048	100β → 102β	26	NCS p_x	Fe d_{yz}	NCS → Fe^{IV} CT
				98β → 102β	24	O p_x	Fe d_{yz}	O → Fe^{IV} CT
				99β → 103β	15	O p_y	Fe d_{xz}	O → Fe^{IV} CT
	10	18 700	0.00225	102α → 104α	37	NCS p_x	Fe $d_{x^2-y^2}$	NCS → Fe^{IV} CT
				100α → 104α	18	Fe d_{yz}	Fe $d_{x^2-y^2}$	Fe^{IV} d → d
				101α → 105α	17	Fe d_{xz}	Fe d_{z^2}	Fe^{IV} d → d
				103α → 105α	12	NCS p_y	Fe d_{z^2}	NCS → Fe^{IV} CT
	11	18 800	0.00273	103α → 104α	39	NCS p_y	Fe $d_{x^2-y^2}$	NCS → Fe^{IV} CT
				101α → 104α	23	Fe d_{xz}	Fe $d_{x^2-y^2}$	Fe^{IV} d → d
				100α → 105α	12	Fe d_{yz}	Fe d_{z^2}	Fe^{IV} d → d
iii	18	22 900	0.17611	100β → 103β	53	NCS p_x	Fe d_{xz}	NCS → Fe^{IV} CT
				101β → 102β	34	NCS p_y	Fe d_{yz}	NCS → Fe^{IV} CT
iv	29	31 400	0.00551	93β → 103β	49	O p_z	Fe d_{xz}	O → Fe^{IV} CT
				100β → 105β	17	NCS p_x	Fe d_{z^2}	NCS → Fe^{IV} CT
				99α → 104α	14	N_{TMC} p	Fe $d_{x^2-y^2}$	N_{TMC} → Fe^{IV} CT
	30	32 300	0.07302	99α → 104α	47	N_{TMC} p	Fe $d_{x^2-y^2}$	N_{TMC} → Fe^{IV} CT
				93β → 103β	10	O p_z	Fe d_{xz}	O → Fe^{IV} CT
	32	33 000	0.04030	98α → 104α	28	N_{TMC} p	Fe $d_{x^2-y^2}$	N_{TMC} → Fe^{IV} CT
				97α → 105α	18	Fe d_{xy}	Fe d_{z^2}	Fe^{IV} d → d
				97β → 105β	12	Fe d_{xy}	Fe d_{z^2}	Fe^{IV} d → d

[a]Energies have been rounded to the nearest 100 cm^{-1}.

Table S20. Energies (eV) and Compositions (%) of the Fe 3d-, O 2p-, N 2p-Based MOs from Spin-Unrestricted PBE0 DFT Computations Performed on a Model of $[Fe^{IV}(O)(TMC)(N_3)]^+$.

orbital	description	occup	spin	energy	Fe 3d	Fe 4p	O 2p	N_{axial} 2p	N_{TMC} 2p
93	Fe d_{xy}	1.0	↑	-12.1338	79.3	0.1	1.2	0.5	6.3
94	N_{TMC} 2p	1.0	↑	-11.7604	6.9	7.1	10.2	2.6	38.5
95	N_{TMC} 2p	1.0	↑	-11.6269	8.4	6.7	13.7	1.9	31.8
96	Fe d_{yz}	1.0	↑	-10.7099	17.1	0.4	50.0	1.3	16.8
97	Fe d_{xz}	1.0	↑	-10.6362	15.5	0.2	53.6	2.6	16.0
98	N_3 $p_{y/z}$	1.0	↑	-9.6609	4.3	1.1	5.7	81.6	0.7
99	N_3 p_x	1.0	↑	-9.4031	5.1	0	1.8	87.2	0.8
100	Fe $d_{x^2-y^2}$	0.0	↑	-6.0837	62.5	0	0	0	25.0
101	Fe d_{z^2}	0.0	↑	-5.0642	50.7	0.7	18.8	8.8	10.1
93	Fe d_{xy}	1.0	↓	-11.1777	92.1	0.1	1.6	0.1	1.6
94	O $2p_x$	1.0	↓	-10.9530	33.6	0.2	38.2	9.1	8.1
95	O p_y	1.0	↓	-10.8701	37.3	0.5	36.7	7.3	7.7
96	N_3 $p_{y/z}$	1.0	↓	-9.5900	1.4	1.0	11.2	76.5	2.5
97	N_3 p_x	1.0	↓	-9.3590	0.1	0.3	8.8	79.4	3.4
98	Fe d_{yz}	0.0	↓	-5.5247	54.9	0.4	35.7	3.1	0.6
99	Fe d_{xz}	0.0	↓	-5.3399	60.7	0.4	27.6	7.5	0.6
100	Fe $d_{x^2-y^2}$	0.0	↓	-4.6866	75.0	0	0.1	0	14.7
101	Fe d_{z^2}	0.0	↓	-4.2004	54.9	0.9	16.4	8.9	7.3

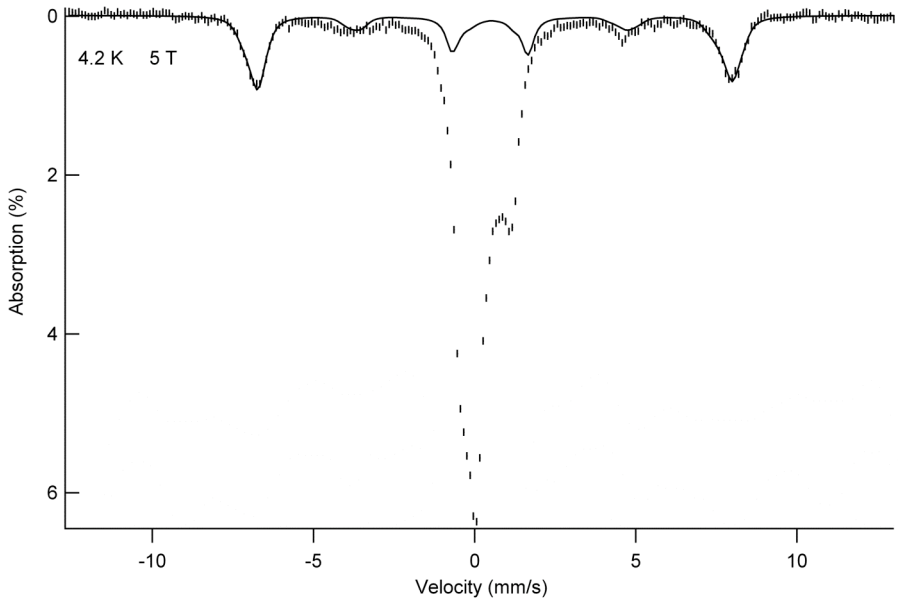

Figure S1. Mössbauer spectrum of $[Fe^{IV}(O)(TMC)(N_3)]^+$ recorded at 4.2 K in an applied field of 5.0T. Solid line shows a simulation of a high-spin ferric contaminant.

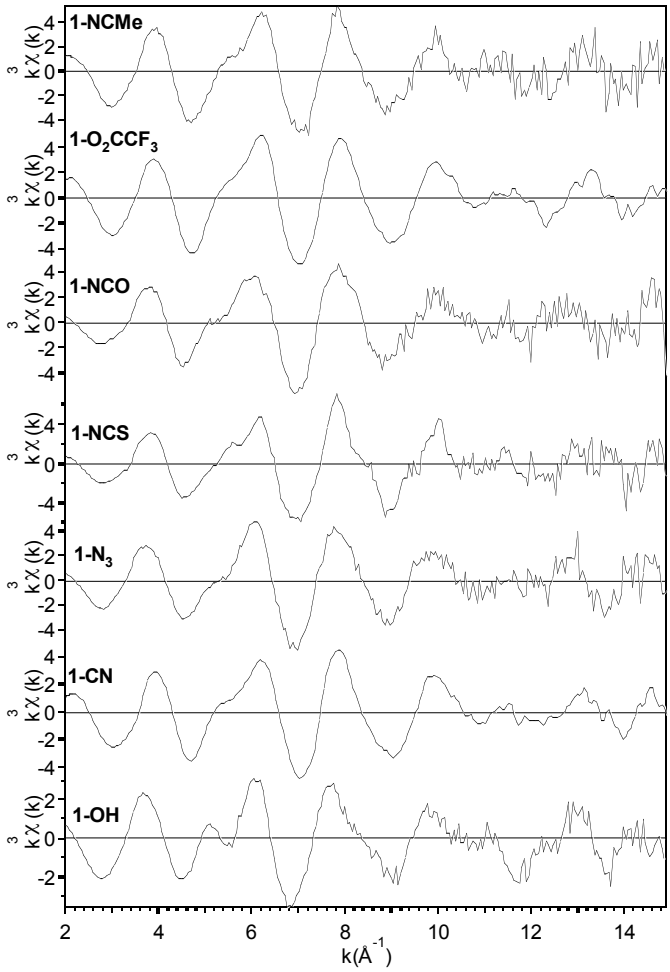

Figure S2. Unfiltered EXAFS data collected for $[Fe^{IV}(O)(TMC)(NCMe)]^{2+}$ (**1**-NCMe), $[Fe^{IV}(O)(TMC)(O_2CCF_3)]^{+}$ (**1**-O_2CCF_3), $[Fe^{IV}(O)(TMC)(NCO)]^{+}$ (**1**-NCO), $[Fe^{IV}(O)(TMC)(NCS)]^{+}$ (**1**-NCS), $[Fe^{IV}(O)(TMC)(N_3)]^{+}$ (**1**-N_3), $[Fe^{IV}(O)(TMC)(CN)]^{+}$ (**1**-CN), $[Fe^{IV}(O)(TMC)(OH)]^{+}$ (**1**-OH).

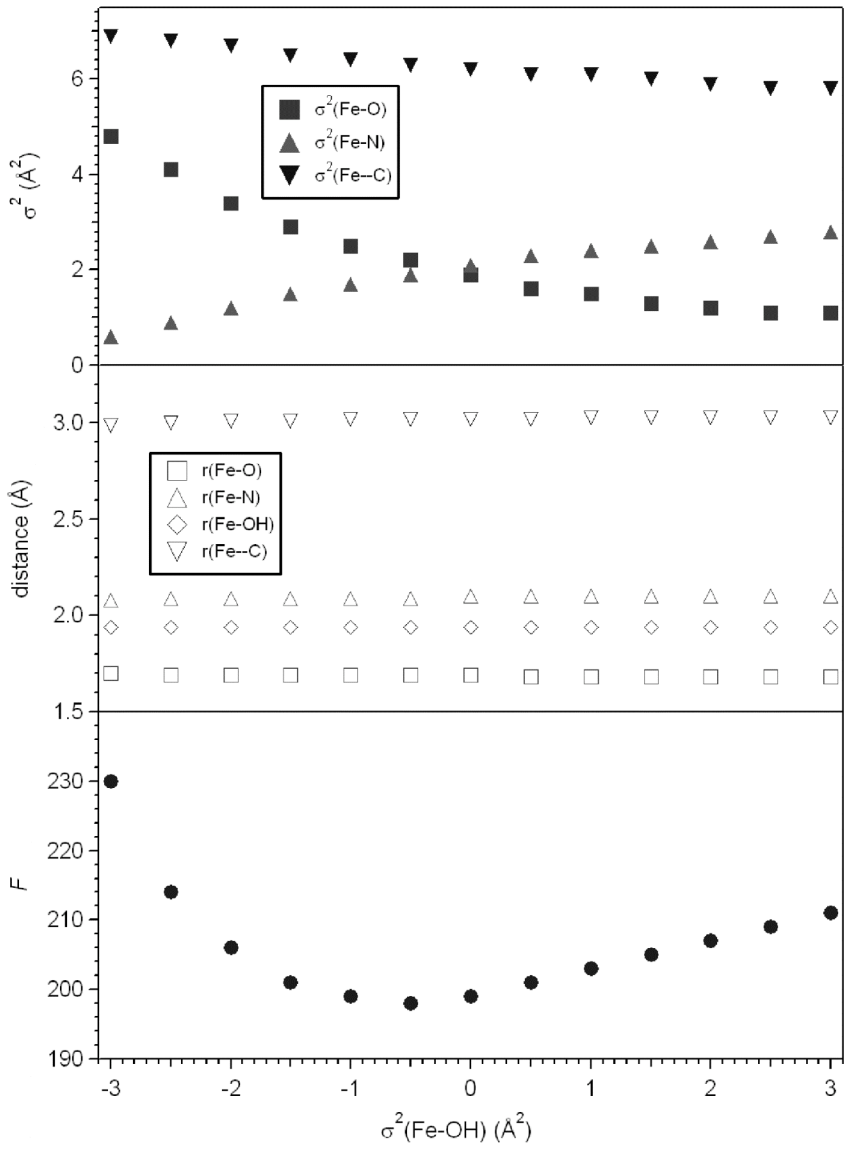

Figure S3. Plot of EXAFS fitting parameters σ^2 (Å^2) and iron-scatterer distance (Å) (top and center) as well as the goodness-of-fit parameter F x 10^3 (bottom) as a function of σ^2(Fe–OH) for $[Fe^{IV}(O)(TMC)(OH)]^+$.

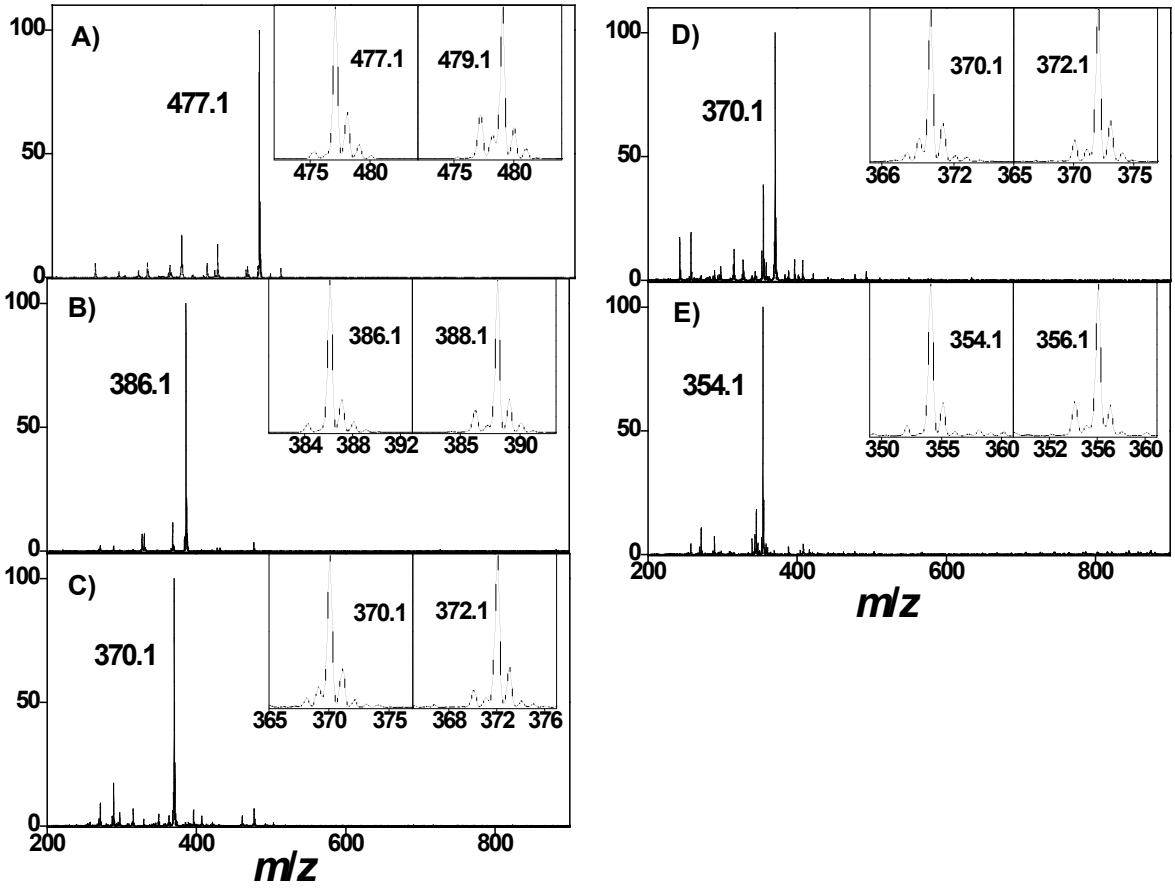

Figure S4. Electrospray ionization mass spectra of $[Fe^{IV}(O)(TMC)(X)]^+$; (A) CH_3CN, (B) NCS^-, (C) N_3, (D) NCO^-, and (E) CN^- in CH_3CN at 25°C. Insets show observed isotope distribution patterns for $[Fe^{IV}(^{16}O)(TMC)(X)]^+$ (left panel) and $[Fe^{IV}(^{18}O)(TMC)(X)]^+$ (right panel).

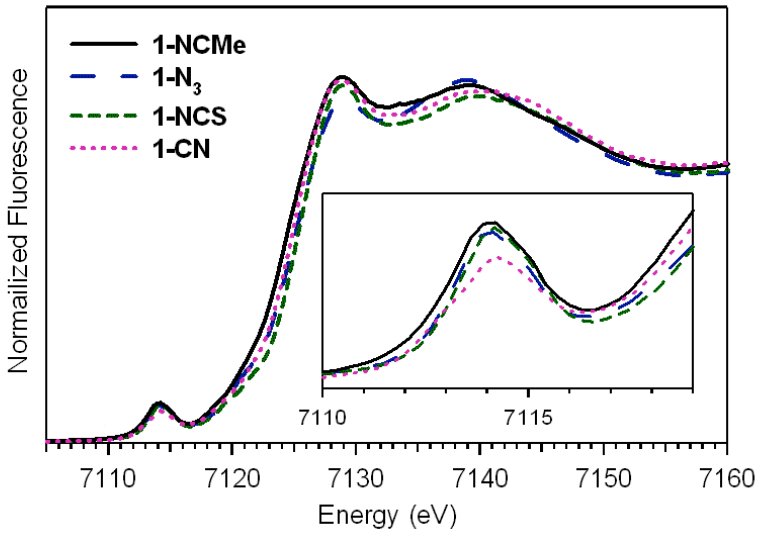

Figure S5. Fe K-edge X-ray absorption near-edge structures of $[Fe^{IV}(O)(TMC)(NCMe)]^+$ (—), $[Fe^{IV}(O)(TMC)(N_3)]^+$ (——), $[Fe^{IV}(O)(TMC)(NCS)]^+$ (---), and $[Fe^{IV}(O)(TMC)(CN)]^+$ (▪▪▪) obtained at 10 K.

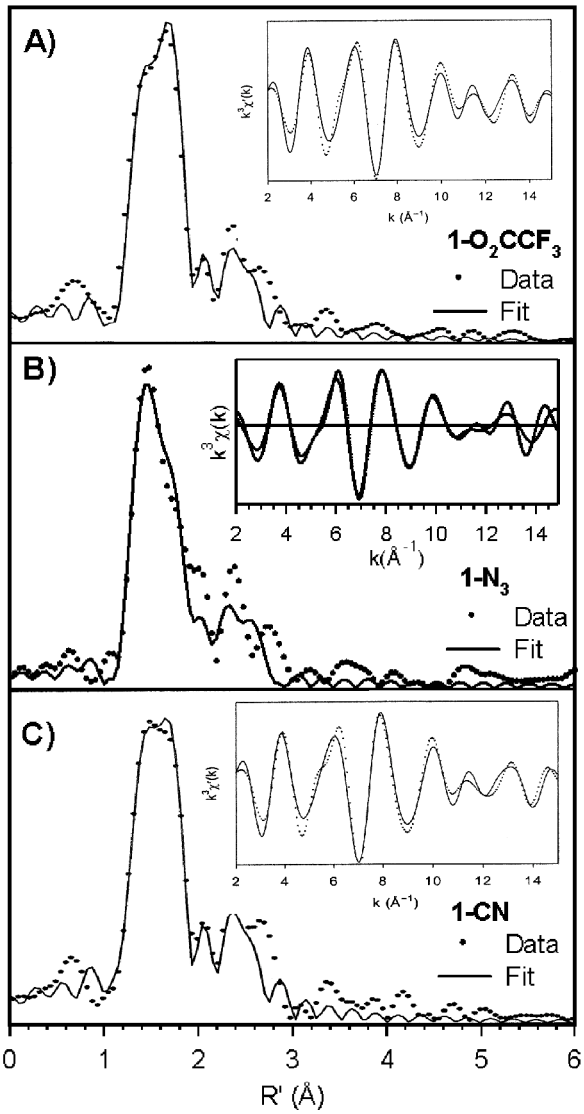

Figure S6. Fourier transforms of Fe K-edge EXAFS data [$k^3\chi(k)$] and Fourier-filtered EXAFS spectra (insets), experimental data (···) and fits (—) for A) $[Fe^{IV}(O)(TMC)(O_2CCF_3)]^{2+}$ (**1**-O_2CCF_3), B) $[Fe^{IV}(O)(TMC)(N_3)]^{+}$ (**1**-N_3), and C) $[Fe^{IV}(O)(TMC)(CN)]^{+}$ (**1**-CN). Details regarding the EXAFS fits are given in Tables 3 and S2.

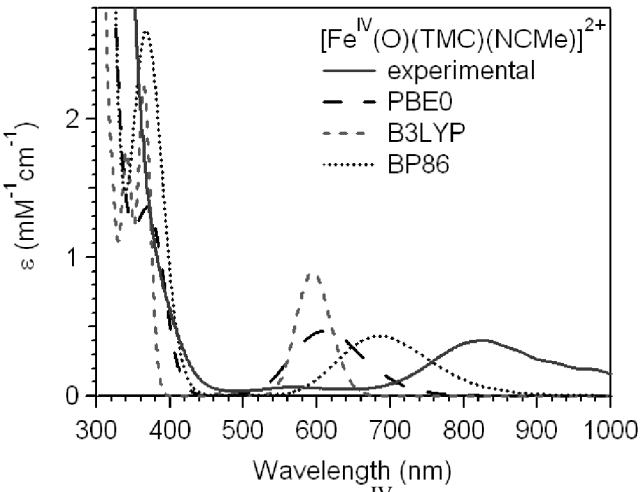

Figure S7. Experimental absorption spectrum of $[Fe^{IV}(O)(TMC)(NCMe)]^{2+}$ (**1**-NCMe) and TD-DFT computed absorption spectra predicted for a geometry optimized model of **1**-NCMe using the PBE0, B3LYP, and BP86 density functionals.

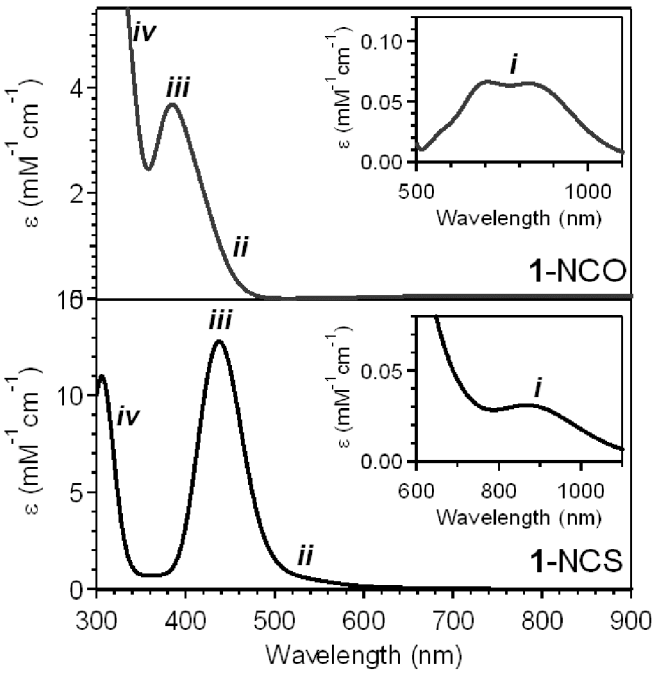

Figure S8. TD-DFT computed absorption spectra predicted for a geometry optimized models of **1**-NCO (top) and **1**-NCS (bottom) using the PBE0 functional.